doi:10.1016/j.jmb.2008.11.038 J. Mol. Biol. (2009) 385, 1277–1286

JMB

Available online at www.sciencedirect.com

ScienceDirect

ELSEVIER

Nanomechanical Properties of Tenascin-X Revealed by Single-Molecule Force Spectroscopy

Ashlee Jollymore[1], Claire Lethias[2], Qing Peng[1], Yi Cao[1] and Hongbin Li[1]*

[1]*Department of Chemistry, University of British Columbia, Vancouver, BC, V6T 1Z1, Canada*

[2]*Institut de Biologie et Chimie des Prote'ines, IFR 128 Biosciences Lyon-Gerland, CNRS UMR 5086, Universite' de Lyon, 7 Passage du, Vercors, 69367 Lyon Cedex 07, France*

Received 26 August 2008; received in revised form 10 November 2008; accepted 18 November 2008
Available online
27 November 2008

Tenascin-X is an extracellular matrix protein and binds a variety of molecules in extracellular matrix and on cell membrane. Tenascin-X plays important roles in regulating the structure and mechanical properties of connective tissues. Using single-molecule atomic force microscopy, we have investigated the mechanical properties of bovine tenascin-X in detail. Our results indicated that tenascin-X is an elastic protein and the fibronectin type III (FnIII) domains can unfold under a stretching force and refold to regain their mechanical stability upon the removal of the stretching force. All the 30 FnIII domains of tenascin-X show similar mechanical stability, mechanical unfolding kinetics, and contour length increment upon domain unfolding, despite their large sequence diversity. In contrast to the homogeneity in their mechanical unfolding behaviors, FnIII domains fold at different rates. Using the 10th FnIII domain of tenascin-X (TNXfn10) as a model system, we constructed a polyprotein chimera composed of alternating TNXfn10 and GB1 domains and used atomic force microscopy to confirm that the mechanical properties of TNXfn10 are consistent with those of the FnIII domains of tenascin-X. These results lay the foundation to further study the mechanical properties of individual FnIII domains and establish the relationship between point mutations and mechanical phenotypic effect on tenascin-X. Moreover, our results provided the opportunity to compare the mechanical properties and design of different forms of tenascins. The comparison between tenascin-X and tenascin-C revealed interesting common as well as distinguishing features for mechanical unfolding and folding of tenascin-C and tenascin-X and will open up new avenues to investigate the mechanical functions and architectural design of different forms of tenascins.

Keywords: tenascin; single molecule force spectroscopy; mechanical unfolding; FnIII domains

Edited by S. Radford

Introduction

Tenascins are a family of highly conserved oligomeric glycoproteins in the extracellular matrix (ECM) of vertebrate organisms.[1–4] Tenascins are involved in the process of mechanotransduction and play important roles in modulating cell adhesion as well as cell–matrix interactions.[2,5,6] A wide range of ECM molecules including proteins, glycosaminoglycans, and proteoglycans are found to bind to tenascins with high affinity.[3] These adhesive properties of tenascins help knit structural ECM proteins with surrounding cells as well as other ECM components to form an interacting network to provide desired mechanical strength and elasticity to tissues. Mechanical forces are constantly involved during such processes. Thus, understanding how tenascins respond to mechanical stretching force is important to the understanding of biological and mechanical roles of tenascins in such mechanotransduction processes.

There are five known tenascins: tenascin-C, tenascin-R, tenascin-W, tenascin-X, and tenascin-Y.[7] All tenascins share the same tandem modular structure, and the constituent domains can be divided into four

*Corresponding author. E-mail address: Hongbin@chem.ubc.ca.

Abbreviations used: FnIII, fibronectin type III; TNXfn10, 10th FnIII domain of tenascin-X; ECM, extracellular matrix; EGF, epidermal growth factor; AFM, atomic force microscopy; EDS, Ehlers–Danlos syndrome; WLC, worm-like chain.

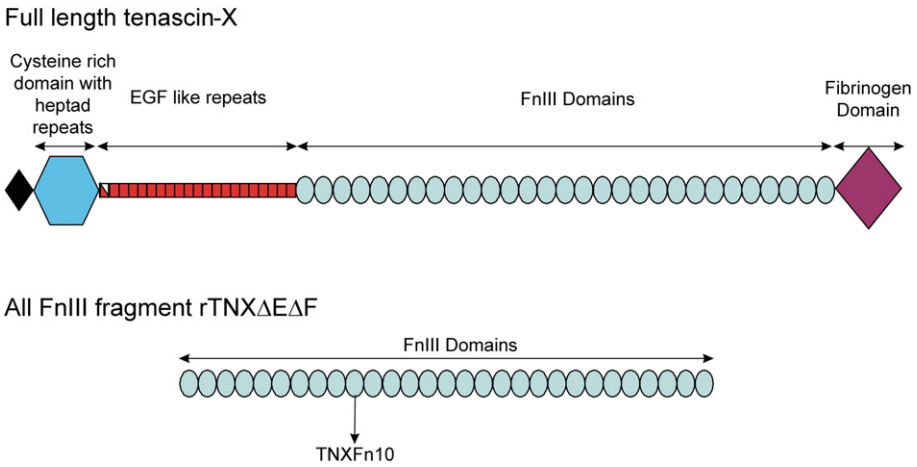

Fig. 1. Schematics of the structure of bovine tenascin-X. (a) Schematic structure of full-length bovine tenascin. Tenascin-X is a tandem modular protein and consists of an N-terminal cysteine-rich domain, a stretch of 18.5 EGF domains, an array of 30 FnIII domains, and a C-terminal fibrinogen-like domain. (b) Schematic structure of truncated tenascin-X (rTNXΔEΔF), which is composed of all the 30 FnIII domains only.

structurally distinct classes: a tenascin-assembly domain, a stretch of epidermal-growth-factor (EGF)-like repeats, a fibronectin type III (FnIII) domain region that is composed of a series of FnIII domains, and a terminal knob domain that is homologous to the globular domain of fibrinogen. Tenascins typically exist as oligomers assembled from tenascin monomers via heptad repeats, further stabilized by disulfide bridges in the tenascin-assembly domain.[8,9] Despite the importance of the mechanical properties of tenascins in their biological functions, tenascin-C is the only form of tenascin whose mechanical properties have been studied in detail using single-molecule atomic force microscopy (AFM).[10–14] Single-molecule AFM studies revealed that tenascin-C is an elastic protein, and its contour length can be extended to several times its resting one by mechanically unfolding its constituting FnIII domains under a stretching force.[10] However, the mechanical properties of other forms of tenascins remain unexplored, and thus, it has not been possible to investigate the mechanical roles of other forms of tenascins or to directly compare the mechanical properties and mechanical design of different forms of tenascins. As a step towards understanding the mechanical properties and design of other forms of tenascins, here we use single-molecule AFM to characterize the mechanical properties of recombinant full-length bovine tenascin-X as well as its fragment.

Tenascin-X is expressed in a wide range of tissues including skin, joints, heart, and blood vessels.[15] Tenascin-X binds a range of molecules in the ECM as well as on the cell membrane[16–18] including collagen fibrils, decorin,[19] and glycosaminoglycans[17] and plays important roles in regulating the structure and mechanical properties of connective tissues. Recently, a recessive form of Ehlers–Danlos syndrome (EDS), an inherited connective disorder, has been found to result from deficiency as well as point mutations in the tenascin-X gene.[20,21] The typical symptoms of EDS are hypermobile joints, hyperelastic skin, and easy bruising. Tenascin-X is the first gene outside the collagen family that causes EDS, highlighting the importance of tenascin-X in the structure and mechanical properties of connective tissues. Similar to other tenascins, bovine tenascin-X has a modular structure (Fig. 1) and is composed of an N-terminal domain, an EGF domain region containing 18.5 EGF domains, an FnIII domain region containing 30 FnIII domains, and a C-terminal fibrinogen-like terminal domain.[22] Using single-molecule AFM, we have stretched bovine tenascin-X molecules to measure their mechanical properties. Our results demonstrate that tenascin-X is an elastic protein, and its FnIII domains can unfold under a stretching force and refold to regain their mechanical stability upon removal of the stretching force. Our results show that tenascin-X and tenascin-C not only share some similar mechanical features but also exhibit distinguishing mechanical properties that are unique to either tenascin-X or tenascin-C. These results pave the way to investigating how the mechanical properties of tenascin-X influence the biological functions of tenascin-X and making it possible to carry out thorough comparative studies among different forms of tenascins to examine how the mechanical properties of tenascins are finely regulated at a molecular level by their similar yet distinctive modular design.

Results

Mechanical unfolding of the full-length tenascin-X and all-FnIII fragment (rTNXΔEΔF)

Using single-molecule AFM,[10,23] we have investigated the mechanical properties of the full-length bovine tenascin-X. The full-length tenascin-X was deposited onto a clean glass coverslip and picked up by the AFM tip randomly along its contour. Stretching tenascin-X between the AFM tip and

glass substrate resulted in force–extension curves exhibiting characteristic sawtooth pattern appearance (Fig. 2a), in which the individual force peaks correspond to the mechanical unfolding events of individually folded domains in tenascin-X and the last peak corresponds to the stretching and subsequent detachment of the polypeptide chain from either the AFM tip or substrate. The number of unfolding force peaks in each individual force–extension curve varies and can be up to 18, indicative of tenascin-X fragment of different lengths being picked up and stretched. The vast majority of the unfolding force peaks are equally spaced with a peak-to-peak spacing of ~24 nm, corresponding to a contour length increment (ΔL_c) of ~28 nm measured by the worm-like chain (WLC) model of polymer elasticity fits (red lines). Many of the force–extension curves also exhibit a long spacer, which can be up to more than 200 nm long, prior to the observed

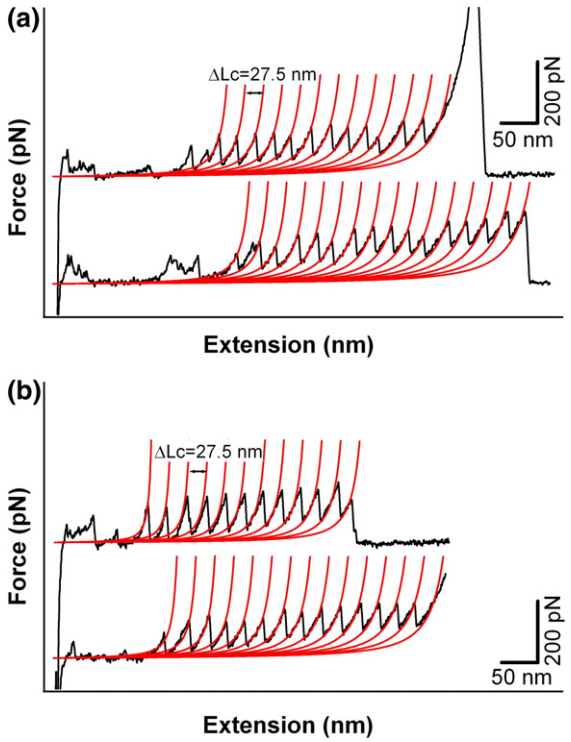

Fig. 2. Force–extension relationships of the full-length bovine tenascin-X (a) and fragment rTNXΔEΔF (b). The force–extension relationships of full-length tenascin-X are characterized by a typical sawtooth pattern appearance with long spacers preceding the unfolding force peaks. The force–extension curves contain varying number of unfolding force peaks, which is up to 18. The vast majority of sawtooth peaks are equally spaced, and WLC fits (red lines) show that unfolding events are of contour length increment (ΔL_c) of ~28 nm, corresponding to the mechanical unfolding of FnIII domains of tenascin-X. The amplitude of the unfolding force peaks of FnIII domains varies around an average value of ~150 pN. Compared with full-length tenascin-X, the mechanical unfolding of rTNXΔEΔF shows similar features. The average unfolding force of FnIII domains in rTNXΔEΔF is ~160 pN, and the length of the spacers preceding the FnIII unfolding events are shorter on average than that of full-length tenascin-X.

sawtooth-like unfolding force peaks. The long spacer can either be featureless or exhibit irregular unfolding force peaks.

To pinpoint the molecular origin of the observed mechanical features in the force–extension curves of the full-length tenascin-X, we also examined the mechanical properties of rTNXΔEΔF, a recombinant fragment of tenascin-X, which only consists of all the FnIII domains of tenascin-X.[18] Stretching rTNXΔEΔF resulted in characteristic sawtooth-like force–extension curves of as many as 17 force peaks, and two typical curves, which contain 12 and 15 equally spaced unfolding force peaks, are shown in Fig. 2b. Since rTNXΔEΔF contains only FnIII domains, the observed unfolding force peaks in rTNXΔEΔF can be ascribed to the mechanical unfolding of FnIII domains without any ambiguity. It is of note that the characteristics of the unfolding force peaks observed for rTNXΔEΔF are very similar to those observed in the full-length tenascin-X, that is, identical ΔL_c and similar unfolding forces. Thus, the unfolding events observed in the force–extension curves of the full-length tenascin-X result from the mechanical unfolding of FnIII domains. In comparison with the full-length tenascin-X, rTNXΔEΔF typically shows shorter spacers preceding the unfolding force peaks in their force–extension curves. Such differences are likely to originate from the contribution to the initial contour length by the series of disulfide-bonded EGF domains as well as other nonstructured amino acid sequences in the full-length tenascin-X, since these domains are highly disulfide bonded and cannot be mechanically unraveled when the stretching force is only a few hundred piconewtons. The unfolding of the terminal fibrinogen-like domain may also contribute to the initial spacer of the full-length tenascin-X.

Since the unfolding force peaks in the full-length tenascin-X and recombinant fragment rTNXΔEΔF correspond to the mechanical unfolding of FnIII domains, here we focus on results from the full-length tenascin-X only for the purpose of convenience. Figure 3a shows the unfolding force histogram of the FnIII domains compiled from different force–extension curves. Since tenascin-X is picked up randomly along its contour, unfolding force peaks of FnIII domains in different force–extension curves result from the unfolding of different FnIII domains in tenascin-X. Considering all 30 FnIII domains are different from each other, the unfolding force histogram shown in Fig. 3a represents an averaged picture of the mechanical stability of all 30 FnIII domains in tenascin-X. The average unfolding force is 148±26 (n=3100). It is of note that although all the 30 FnIII domains are different from each other, the distribution of the unfolding forces of FnIII domains shows a narrow distribution with a standard deviation of 26 pN, suggesting that the majority of FnIII domains unfold at similar unfolding forces and are of similar mechanical stability in their native settings. However, it is important to point out that since different fragments of tenascin-X are picked up during each individual force–exten-

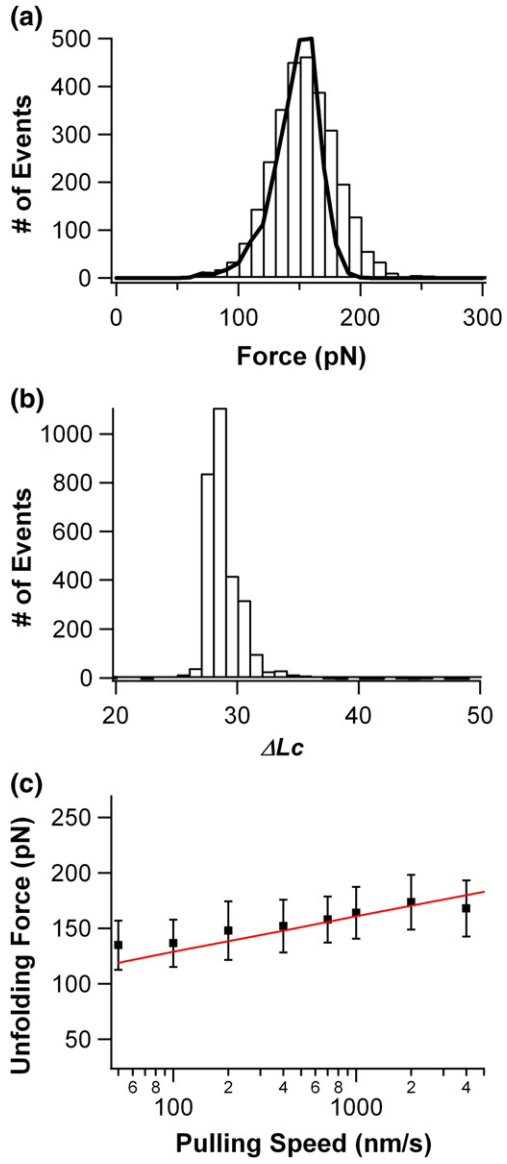

Fig. 3. Average mechanical properties of FnIII domains of tenascin-X under a stretching force. (a) Unfolding force histogram of FnIII domains. Despite the heterogeneity in the sequences of all FnIII domains, the unfolding force histogram shows a narrow distribution with an average unfolding force of 148±26pN. The continuous line is the unfolding force histogram generated by Monte Carlo simulations using α_0 of 9×10^{-5} s^{-1} and Δx_u of 0.34 nm. (b) Histogram of contour length increment of FnIII domains shows a narrow distribution with an average ΔL_c of 28.4±1.7 nm. (c) The mechanical unfolding forces of FnIII domains show a weak dependence on the pulling speed. We found that, using a combination of α_0 of 9×10^{-5} s^{-1} and Δx_u of 0.34 nm, Monte Carlo simulations can reproduce the pulling speed dependence of unfolding forces as well as unfolding force histogram well, indicating that the mechanical unfolding behaviors of the majority of FnIII domains of tenascin-X can be described adequately using an average behavior.

sion curve and that individual FnIII domains may have different probabilities of being picked up and stretched, the mechanical unfolding forces of some FnIII domains may be underrepresented in the narrowly distributed unfolding force histogram.

Fitting the WLC model[24] of polymer elasticity (red lines) to consecutive unfolding events of FnIII domains measures the contour length increment (ΔL_c) of individual FnIII domain upon its mechanical unfolding (Fig. 2a). Although the length of an individual FnIII domain varies from 87 to 134 aa,[22] ΔL_c of individual FnIII domain exhibits a narrow distribution with an average value of 28.4±1.7 nm (Fig. 3b), which is very similar to that for FnIII domains in tenascin-C.[10,11] If we assume that the distance between the N- and C-termini in the folded structure of FnIII domains is between 4 and 6 nm, ΔL_c of ~28 nm would indicate that the folded FnIII domains contain 89 to 94 aa on average [(28 nm + 4 nm)/0.36 nm/aa = 89 aa]. Since there is large variation in the predicted length of FnIII domains, it is likely that the narrow distribution of ΔL_c reflects that the majority of FnIII domains have folded structures that are of a similar number of amino acids. Therefore, the variation in the length of different FnIII domains largely reflects the variation in the length of linker sequences between different FnIII domains, rather than the different number of amino acids in the folded structure of FnIII domains.

Pulling speed dependence of unfolding forces of FnIII domains

To characterize the mechanical unfolding kinetics of FnIII domains of tenascin-X in detail, we carried out the unfolding experiments of full-length tenascin-X at different pulling speeds to measure the pulling speed dependence of the mechanical unfolding forces. As shown in Fig. 3c, the unfolding forces of FnIII domains show a weak dependence on the pulling speed: the unfolding force increases from 130 pN at a pulling speed of 50 nm/s to 170 pN at a pulling speed of 2000 nm/s. Such a weak pulling speed dependence is similar to that observed for the FnIII domains of tenascin-C[10,11] but is in sharp contrast with the strong pulling speed dependence of the unfolding forces for FnIII domains of fibronectin[25] as well as Ig domains from the giant muscle protein titin [23,26] (Fig. 3b). Assuming that all the FnIII domains in tenascin-X share similar unfolding kinetics and unfold in a two-state manner, we used Monte Carlo simulations to estimate the spontaneous unfolding rate constant at zero force (α_0) and the distance between the folded state and the mechanical unfolding transition state (Δx_u). By carrying out Monte Carlo simulations to reproduce the unfolding force histogram as well as its pulling speed dependence, we found that a combination of 0.34 nm for Δx_u and 9×10^{-5} s^{-1} for α_0 can describe the unfolding force distribution (Fig. 3a) as well as pulling speed dependence of unfolding forces well (Fig. 3c).

Folding kinetics of FnIII domains

By repeatedly stretching and relaxing the same tenascin-X molecule, it is possible to directly mea-

sure the folding kinetics of FnIII domains at the single-molecule level.[26] Figure 4a shows such a representative stretching-relaxation experiment on a tenascin-X molecule obtained using double-pulse protocols. In the first pulse, we stretched and completely unfolded the FnIII domains contained in the tenascin-X fragment being picked up (trace 1). By counting the number of unfolding force peaks of FnIII domains (N_{total}), we will know the number of FnIII domains in this particular tenascin-X fragment. The completely unfolded polyprotein chain was then quickly relaxed to zero extension (trace 2) to allow the unfolded FnIII domains to refold for a fixed period of time Δt. We then stretched the molecule again to measure its force–extension profile (trace 3). The number of unfolding force peaks that appeared in the subsequent force–extension curve measures the number of FnIII domains (N_{refold}) that have managed to refold and regain their mechanical stability within relaxation time Δt. By changing the relaxation time Δt, we can directly measure the folding kinetics by plotting the probability of folding (N_{total}/N_{refold}) *versus* relaxation time Δt (Fig. 4b). It is evident that the longer the relaxation time Δt, the more FnIII domains can refold and regain their mechanical stability. Almost all the FnIII domains can refold after 2 s. The time course of the folding of FnIII domains of tenascin-X can be described well by a double exponential model, $(N_{refold}/N_{total})=A(1-e^{-\beta_1 t})+(1-A)(1-e^{-\beta_2 t})$, where N_{refold}/N_{total} is the folding probability of FnIII domains at a relaxation time t and β_1 and β_2 correspond to the folding rate constants. We found that, on average, 60% of FnIII domains fold with a rate constant of 22 s^{-1} and 40% of FnIII domains fold at a rate of 3 s^{-1}. Considering the heterogeneous nature of the FnIII domains, we attribute the biphasic folding kinetics to heterogeneity in folding kinetics among the different FnIII domains of tenascin-X.

Mechanical unfolding and folding dynamics of the 10th FnIII domain of tenascin-X

Although we have characterized the mechanical unfolding and folding dynamics of the FnIII domains of tenascin-X using AFM, the information we obtained is an averaged property of all the FnIII domains of tenascin-X due to the inherent sequence heterogeneity among the 30 different FnIII domains of tenascin-X. To obtain information about the folding and unfolding dynamics of individual FnIII domains in detail, one will need to investigate the mechanical unfolding and folding dynamics of FnIII domains one at a time. Here, we chose the 10th FnIII domain of tenascin-X (TNXfn10) as a model system to illustrate some of the general features among the FnIII domains. To facilitate the mechanical characterization of TNXfn10 using single-molecule AFM, we constructed a heteropolyprotein $(GB1\text{-}TNXfn10)_4$ (Fig. 5a), in which GB1 domains alternate with TNXfn10 domains and the well-characterized GB1 domains, with ΔL_c of ~18 nm and unfolding force of ~180 pN, serve as a mechanical fingerprint[27,28] for identifying the mechanical features of TNXfn10. Stretching $(GB1\text{-}TNXfn10)_4$ results in characteristic sawtooth-like force–extension curves of two types of unfolding events with clearly different ΔL_c values (Fig. 5b): unfolding events occurring at the beginning of the force–extension curves tend to show ΔL_c of ~28 nm (colored green), while those occurring towards the end of the force–extension curves tend to show ΔL_c of ~18 nm (colored red). The unfolding events of ΔL_c of ~18 nm correspond to the unfolding of GB1 domains in the heteropolyprotein, while the unfolding events of ΔL_c of ~28 nm correspond to the unfolding of TNXfn10. Figure 5c shows the unfolding force histogram of TNXfn10 with an average force of 170±22pN. It seems that the average unfolding force of TNXfn10 is slightly higher than the average unfolding force of FnIII

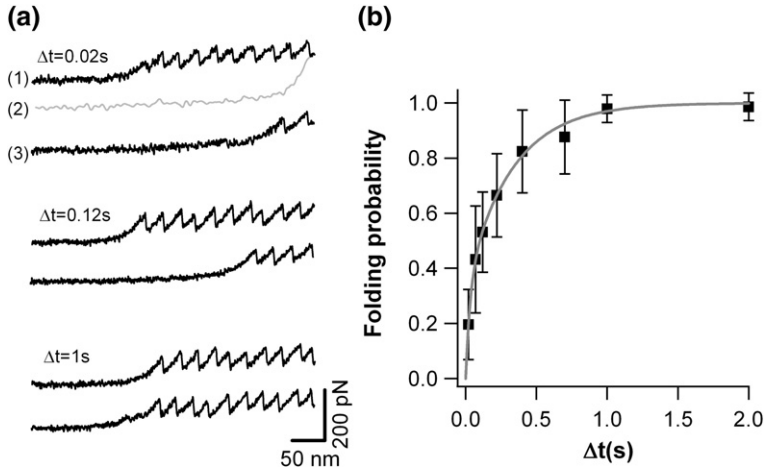

Fig. 4. Mechanical folding kinetics of FnIII domains of tenascin-X. (a) The folding kinetics of FnIII domains can be measured using a double-pulse protocol. In the first pulse, tenascin-X was picked up and stretched to unfold all the FnIII domains in the fragment being picked up. The number of unfolding force peaks allows us to count the number of FnIII domains present in the fragment (trace 1). After complete unfolding, the unfolded protein chain was quickly relaxed to zero extension (trace 2) and allowed to refold at zero extension for time Δt. Then, the protein was stretched again and the number of unfolding force peaks in the resultant force–extension curve (trace 3) indicates the number of FnIII domains that managed to refold within relaxation time Δt. By varying the relaxation time Δt, the folding kinetics of FnIII domains of tenascin-X can be measured. (b) Folding kinetics of FnIII domains. The profile of folding probability of FnIII domains (N_{refold}/N_{total}) *versus* relaxation time (Δt) can be described by a double exponential distribution with a folding rate constant of 22 s^{-1} for the fast phase and 3 s^{-1} for the slow phase.

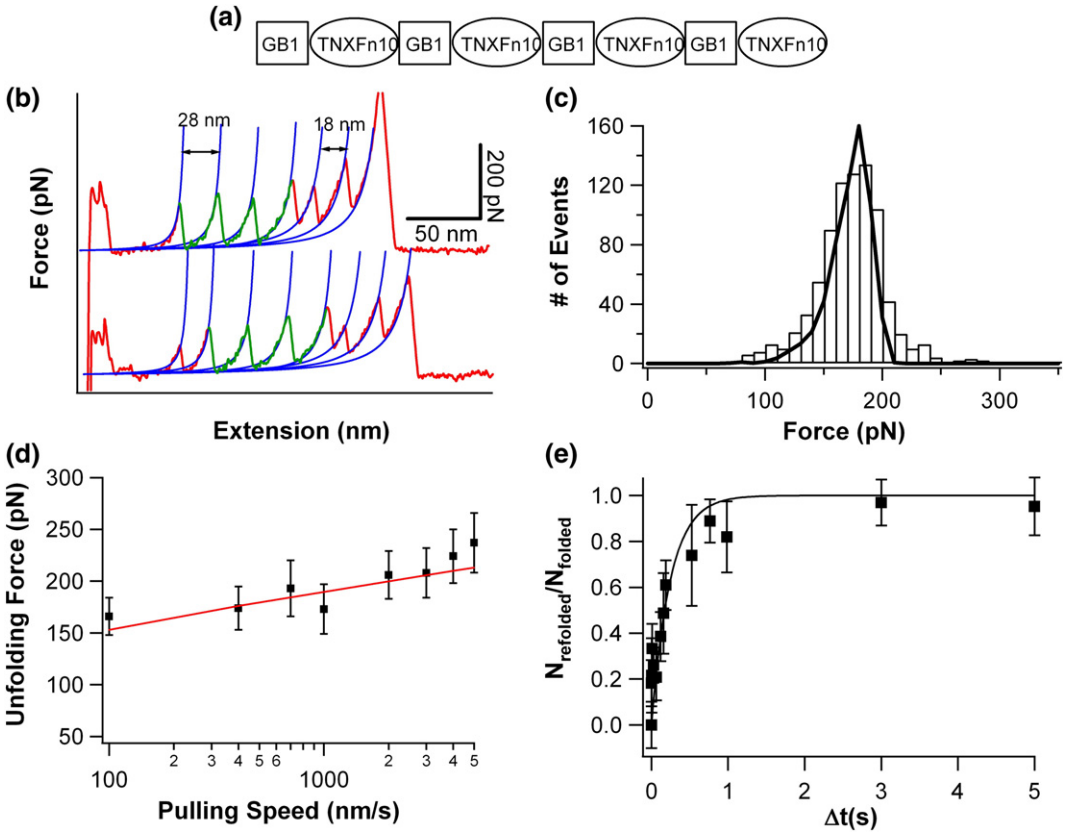

Fig. 5. Mechanical unfolding properties of TNXFn10. (a) Schematics of the heteropolyprotein $(GB1\text{-}TNXFn10)_4$. In the heteropolyprotein, TNXFn10 alternates with the well-characterized GB1 domains, which serve as a fingerprint for identifying single-molecule stretching events. (b) Typical force–extension curves of heteropolyprotein $(GB1\text{-}TNXFn10)_4$. The unfolding force peaks exhibit two different kinds of ΔL_c. The unfolding events with ΔL_c of ~18 nm (colored red) typically occur towards the end of the force–extension curves and correspond to the mechanical unfolding of GB1 domains; the unfolding events with ΔL_c of ~28 nm (colored green) typically occur at the beginning of the force–extension curves and correspond to the mechanical unfolding of TNXfn10 domains. Blue lines are WLC fits to the experimental data. (c) Unfolding force histogram of TNXfn10 domains. The continuous line is the Monte Carlo simulation fit using α_0 of $9\times10^{-5}\ s^{-1}$ and Δx_u of 0.34 nm. (d) Pulling Speed dependence of the unfolding forces of TNXfn10. The continuous line is the Monte Carlo simulation fit using the same parameters as in (c). (e) Folding kinetics of TNXfn10 domains at zero force. The folding kinetics of TNXfn10 can be well described by a single exponential distribution with a folding rate constant of $3\ s^{-1}$.

domains measured in tenascin-X. Mechanical unfolding force of proteins depends on the effective loading rate. Compared with the full-length tenascin-X, the contour length of heteropolyprotein $(GB1\text{-}TNXfn10)_4$ is much shorter, and thus, the effective loading rate for $(GB1\text{-}TNXfn10)_4$ is higher than that for the full-length tenascin-X. Therefore, it is not surprising that the unfolding force of TNXfn10 in a shorter polyprotein is higher than the average unfolding force of FnIII domains in a much longer tenascin-X at the same pulling speed. To determine Δx_u and α_0 for TNXfn10, we also measured the pulling speed dependence of the unfolding forces of TNXfn10 in $(GB1\text{-}TNXfn10)_4$ (Fig. 5d). By fitting the unfolding force distribution as well as its dependence on pulling speed, we found that the parameters used to describe the average behaviors of FnIII domains in tenascin-X can also describe the mechanical unfolding of TNXfn10 adequately. This result is consistent with the conclusion that the majority of FnIII domains show similar mechanical unfolding kinetics (similar α_0 and Δx_u). Using a similar double-pulse protocol, we also measured the folding kinetics of TNXfn10 at zero force (Fig. 5e). It is evident that the time course of the folding of TNXfn10 can be readily described by a single exponential distribution with a folding rate constant β of $3\ s^{-1}$, which is well within the range of the average folding rate constants measured for all the FnIII domains in the full-length tenascin-X. From the combined results on the mechanical unfolding and folding dynamics of TNXfn10, it becomes evident that TNXfn10 can serve as a model system for describing the average behavior of all the FnIII domains in tenascin-X.

Discussion

Tenascins are a family of elastic proteins

Using single-molecule AFM, we have characterized the mechanical unfolding and folding kinetics of

tenascin-X in detail. Our results showed that tenascin-X is an elastic protein and its constitutive FnIII domains can undergo reversible unfolding–folding transitions under a stretching force to effectively modulate the contour length of tenascin-X molecules. These results provide a general and average description of the mechanical properties of tenascin-X and provide the possibility to compare the mechanical behaviors of different forms of tenascins.

Tenascins are a family of highly conserved ECM proteins. The five known tenascins (tenascin-C, tenascin-R, tenascin-W, tenascin-X, and tenascin-Y) are of similar architectures, despite their low sequence homology. FnIII domains are major components of tenascins and are the primary candidates for providing unfolding-regulated elasticity. Tenascin-C is the only tenascin whose elastic behaviors have been investigated in detail previously.[10–12] Although the mechanical properties of tenascin-R, tenascin-W, and tenascin-Y remain to be examined, the AFM results on tenascin-C and tenascin-X suggest that other tenascins are also likely to be elastic proteins and the unfolding of their constituting FnIII domains will be the primary source for domain unfolding mediated elasticity. Since the EGF domains are highly disulfide bonded, they are unlikely to unfold by stretching forces of the amplitude of a few hundreds piconewtons. Thus, EGF domains will remain folded and contribute to the initial contour length of tenascins. It was proposed that the reversible unfolding of FnIII domains in tenascin-C may effectively extend the lifetime of adhesion bonds mediated by tenascin-C.[10] Tenascin-X and other forms of tenascins are also involved in adhesive interactions with a wide range of interacting partners; for example, tenascin-X can bind heparin,[29] decorin,[19] and collagen fibrils[30] and help to provide desired mechanical strength and elasticity to connective tissues as well as regulate the fine structure of connective tissues. Hence, it is possible that the mechanism proposed for tenascin-C also applies to different tenascins, including tenascin-X (e.g., the unfolding of FnIII domains can help to promote tenascin-involved adhesion bonds). However, the general role of delicately designed tenascin mechanics in biological functions is yet to be elucidated. Single-molecule AFM studies on tenascins provide fundamental knowledge of the mechanical proprieties of tenascins, which will be necessary for further studies.

Although our studies on the full-length tenascin-X provide valuable information about the overall behavior of tenascin-X, detailed information on individual FnIII domains can only be obtained by investigating them individually. Our study on TNXfn10 is such an effort. Continued experimental efforts in investigating the mechanical properties of other FnIII domains will be critical to elucidating the molecular determinants of the mechanical stability of FnIII domains and pave the way to evaluate the mechano-phenotypic effect of disease-causing mutations, such as those found in a few FnIII domains and linked to connective disorders.[20,21] Furthermore, these studies will also be of critical importance to directly probe the effect of ligand binding, such as the binding of heparin and decorin to tenascin-X, on the mechanical properties of FnIII domains as well as full-length tenascin-X.

Comparison of the mechanical features of FnIII domains between tenascin-X and tenascin-C

Comparing the mechanical features of the FnIII domains from tenascin-X with those from tenascin-C, we have observed some interesting common as well as distinguishing features in their mechanical properties. FnIII domains from both tenascins exhibit homogeneity in their mechanical unfolding kinetics as well as heterogeneity in their folding kinetics. Despite the sequence diversity across different FnIII domains in tenascin-C or tenascin-X, FnIII domains originating from the same tenascin show surprisingly similar mechanical stability and unfolding kinetics. This behavior is in sharp contrast with the significantly different mechanical stability observed in the constitutive FnIII domains of fibronectin.[25] Since the homology among FnIII domains in tenascin-X (or tenascin-C) is not that different from that for FnIII domains in fibronectin, it is possible that similar mechanical stability among FnIII domains in tenascin-C (or tenascin-X) is a unique feature evolved in FnIII domains of tenascins. Decoding secrets of the mechanical design of FnIII domains that lead to distinct mechanical stability of FnIII domains in tenascin-C and tenascin-X will be critical for tailoring the mechanical stability of FnIII domains in a rational fashion. Steered molecular dynamics simulations will be of tremendous importance in this aspect, as evidenced by the efforts in elucidating mechanical design of FnIII domains in fibronectin.[31–33] In contrast to the homogeneity in their mechanical stability, individual FnIII domains from both tenascin-C and tenascin-X exhibit diverse folding kinetics, which is manifested in their double exponential folding kinetics. It was proposed that different folding kinetics is a mechanism used by nature to prevent misfolding of tandem modular proteins,[34] and the results we obtained here for tenascin-X seems to be consistent with this hypothesis.

Despite the self-similarity in the mechanical stability of the FnIII domains within the same form of tenascin (tenascin-C or tenascin-X), FnIII domains from tenascin-X are consistently stronger than FnIII domains from tenascin-C: the average unfolding force of FnIII domains from tenascin-X is 148 pN, while the average unfolding force of FnIII domains from tenascin-C is ~120–130 pN.[10,13] Considering the low sequence homology among FnIII domains from either tenascin-C or tenascin-X, these results imply that the FnIII domains within the same type of tenascin are likely to have evolved to achieve a self-similarity in their mechanical stability and at the same time to retain their distinct mechanical identity between different types of tenascins. Based on the results on tenascin-C and tenascin-X, we hypothe-

size that FnIII domains from different tenascins may encode distinct mechanical stabilities and thus entail different mechanical functions for different tenascins. Understanding the underlying molecular mechanism will shed light on the architectural design of tenascins and make it possible to use statistical analysis to understand how the mechanical stability of FnIII domains is determined at the molecular level and thus make it possible to tune the mechanical stability of FnIII domains rationally, which will be key to bioengineering of artificial tenascins with tailored mechanical properties.

Another notable difference between tenascin-X and tenascin-C lies in their significant difference in the misfolding frequency of FnIII domains. It was reported that,[13,35] after mechanical unfolding, 90% of FnIII domains in tenascin-C were able to refold correctly, while 10% of neighboring FnIII domains were observed to misfold into dimeric misfolded states at a frequency of ~10%, giving rise to the so-called "skip" in force–extension curves shown in Fig. 6a with Δskip of ~60 nm, which is slightly bigger than twice of the ΔL_c of correctly folded FnIII domains.[13,35] In contrast, the folding of FnIII domains in tenascin-X appears to be much more robust (Fig. 6b): in more than 500 refolding events, we only observed 2 putative misfolding events. The sharp contrast in the folding fidelity of FnIII domains between tenascin-X and tenascin-C raises the question how the folding fidelity of such similar tandem modular proteins is controlled at the amino acid sequence level. It was proposed that high sequence homology is likely a cause for misfolding and aggregation in tandem modular proteins.[34] However, sequence homology between FnIII domains in tenascin-X is not different from that of tenascin-C, suggesting that sequence homology or identity alone is not sufficient to explain the folding fidelity. Hence, FnIII domains from tenascin-C and tenascin-X may represent valuable model systems to examine the potential molecular determinants underlying the folding fidelity of elastomeric proteins as well as their potential biological significance.

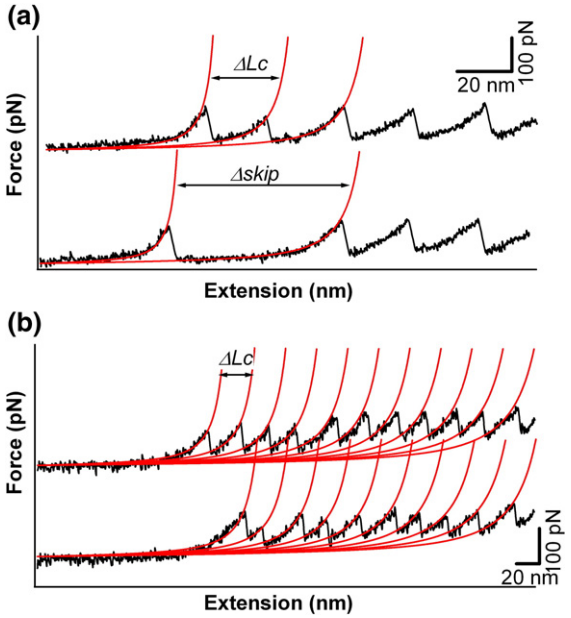

Fig. 6. FnIII domains of tenascin-X show high fidelity in folding. (a) Refolding traces of tenascin-C show misfolding events. After mechanical unfolding, about 10% of FnIII domains of tenascin-C can refold with their neighboring FnIII domains to form a misfolded state, which give rise to Δskip of ~60 nm, which is slightly bigger than twice the ΔL_c observed for the individual correctly folded FnIII domains. (b) Typical refolding traces of tenascin-X. After mechanical unfolding, FnIII domains refold to regain their mechanical stability and show ΔL_c that is identical with that of FnIII domains upon their first unfolding.

Conclusion

We have used single-molecule AFM to characterize the elastic behaviors of full-length tenascin-X as well as its fragment comprising all the FnIII domains. Our results revealed that tenascin-X is an elastic protein and its FnIII domains can undergo reversible unfolding–folding reactions. The folding and unfolding behaviors of FnIII domains exhibit intriguing similarities and distinct contrasts between FnIII domains from tenascin-C and tenascin-X. We hypothesize that different tenascins encode distinct mechanical stability necessary for their different biological functions. These results will pave the way for further studies to investigate how the mechanical properties of tenascin-X regulate their biological functions and how mechanical performance of tenascin-X will respond to disease-causing mutations found in tenascin-X.

Materials and Methods

Protein engineering

Recombinant full-length bovine tenascin-X and a truncated form comprising all its FNIII domains (rTNXΔEΔF) were prepared as described previously.[18] Both proteins were produced by HEK293 cells and secreted in the culture medium. Purification was achieved by two chromatographic steps, the first one by affinity with heparin and the second one on Q-Sepharose.

TNXfn10 gene was amplified from a plasmid encoding TNXfn9–11 via standard polymerase chain reaction using sense primer (CGT GGA TCC CTG CTC TTT GGC ATC CAA GAT) and antisense primer (CCC TCA AAA CCA CGT CTG GGG AGA TCT TAA TAG GGT ACC GAG) and confirmed by direct DNA sequencing. These primers were designed to contain 5′ BamHI site and 3′ KpnI and BglII restrictions and overlap 20 aa with neighboring TNXfn9 and TNXfn11 domains, according to the existing information of domain boundaries.[22] This was done to erase any ambiguity surrounding domain annotation, ensuring that the entire 10th domain was represented within the gene fragment, and to eliminate possible effects on the mechanical properties of TNXfn10 due to incorrectly chosen domain boundaries. The gene of polyprotein chimera $(GB1\text{-}TNXfn10)_4$ was then constructed using a

well-established method described elsewhere[27] based on the identity of the sticky ends generated by digesting BamHI and BglII restriction sites. $(GB1\text{-}TNXfn10)_4$ was constructed in cloning vector pUC19 and then subcloned into expression vector pQE80L. Overexpression of the polyprotein chimera was carried out in DH5α strain and purified by Co^{2+} affinity chromatography. The polyprotein chimera was kept at 4 °C in phosphate-buffered saline buffer at a concentration of 870 μg/ml.

Single-molecule AFM

Single-molecule AFM experiments were carried out on a custom-built AFM, which was constructed as described previously.[27] Each individual AFM cantilever was calibrated using the equipartition theorem before and after each AFM experiment. Protein samples were deposited onto a clean glass coverslip covered by phosphate-buffered saline buffer (~50 μl) and allowed to adsorb for approximately 5 min. During AFM experiments, the AFM tip was first brought into contact with the glass coverslip with a contact force of 5 nN. Upon withdrawing the AFM tip from the glass substrate, tenascin fragments or polyproteins were picked up and stretched by the AFM tip due to the nonspecific interactions between the protein and AFM tip. Multiple molecules can be picked up and stretched at the same time. Short molecules will detach first and give rise to the low force peaks and irregular features as those shown at the beginning of the force–extension curves in Fig. 2b.

The contour length increment ΔL_c of FnIII domains of tenascin-X was measured by fitting the WLC model of polymer elasticity to consecutive unfolding force peaks. A persistence length of 0.4–0.9 nm was used during the fitting. The length of the spacer measures the contour length of the fully folded part of the tandem modular protein. The unfolding of FnIII domains was described as a two-state process with force-dependent rate constants. Monte Carlo simulations were carried out according to published procedures.[26]

Acknowledgements

This work is supported by Canadian Institutes for Health Research Operating Grant MOP-81225, Michael Smith Foundation for Health Research, University of British Columbia Health Research Resources Office, Canada Research Chairs Program, and Canadian Foundation for Innovation. H.L. is a Michael Smith Foundation for Health Research Scholar.

References

1. Erickson, H. P. (1993). Tenascin-C, tenascin-R and tenascin-X: a family of talented proteins in search of functions. *Curr. Opin. Cell Biol.* **5**, 869–876.
2. Chiquet-Ehrismann, R. (1995). Tenascins, a growing family of extracellular matrix proteins. *Experientia*, **51**, 853–862.
3. Jones, F. S. & Jones, P. L. (2000). The tenascin family of ECM glycoproteins: structure, function, and regulation during embryonic development and tissue remodeling. *Dev. Dyn.* **218**, 235–259.
4. Hsia, H. C. & Schwarzbauer, J. E. (2005). Meet the tenascins: multifunctional and mysterious. *J. Biol. Chem.* **280**, 26641–26644.
5. Erickson, H. P. (1997). A tenascin knockout with a phenotype. *Nat. Genet.* **17**, 5–7.
6. Chiquet, M. (1999). Regulation of extracellular matrix gene expression by mechanical stress. *Matrix Biol.* **18**, 417–426.
7. Tucker, R. P., Drabikowski, K., Hess, J. F., Ferralli, J., Chiquet-Ehrismann, R. & Adams, J. C. (2006). Phylogenetic analysis of the tenascin gene family: evidence of origin early in the chordate lineage. *BMC Evol. Biol.* **6**, 60.
8. Kammerer, R. A., Schulthess, T., Landwehr, R., Lustig, A., Fischer, D. & Engel, J. (1998). Tenascin-C hexabrachion assembly is a sequential two-step process initiated by coiled-coil alpha-helices. *J. Biol. Chem.* **273**, 10602–10608.
9. Erickson, H. P. & Inglesias, J. L. (1984). A six-armed oligomer isolated from cell surface fibronectin preparations. *Nature*, **311**, 267–269.
10. Oberhauser, A. F., Marszalek, P. E., Erickson, H. P. & Fernandez, J. M. (1998). The molecular elasticity of the extracellular matrix protein tenascin. *Nature*, **393**, 181–185.
11. Rief, M., Gautel, M., Schemmel, A. & Gaub, H. E. (1998). The mechanical stability of immunoglobulin and fibronectin III domains in the muscle protein titin measured by atomic force microscopy. *Biophys. J.* **75**, 3008–3014.
12. Wang, M. J., Cao, Y. & Li, H. B. (2006). The unfolding and folding dynamics of TNfnALL probed by single molecule force-ramp spectroscopy. *Polymer*, **47**, 2548–2554.
13. Cao, Y. & Li, H. B. (2006). Single molecule force spectroscopy reveals a weakly populated microstate of the FnIII domains of tenascin. *J. Mol. Biol.* **361**, 372–381.
14. Ng, S. P., Rounsevell, R. W., Steward, A., Geierhaas, C. D., Williams, P. M., Paci, E. & Clarke, J. (2005). Mechanical unfolding of TNfn3: the unfolding pathway of a fnIII domain probed by protein engineering, AFM and MD simulation. *J. Mol. Biol.* **350**, 776–789.
15. Egging, D. F., van Vlijmen, I., Starcher, B., Gijsen, Y., Zweers, M. C., Blankevoort, L. *et al.* (2006). Dermal connective tissue development in mice: an essential role for tenascin-X. *Cell Tissue Res.* **323**, 465–474.
16. Egging, D., van den Berkmortel, F., Taylor, G., Bristow, J. & Schalkwijk, J. (2007). Interactions of human tenascin-X domains with dermal extracellular matrix molecules. *Arch. Dermatol. Res.* **298**, 389–396.
17. Elefteriou, F., Exposito, J. Y., Garrone, R. & Lethias, C. (1999). Cell adhesion to tenascin-X mapping of cell adhesion sites and identification of integrin receptors. *Eur. J. Biochem.* **263**, 840–848.
18. Lethias, C., Carisey, A., Comte, J., Cluzel, C. & Exposito, J. Y. (2006). A model of tenascin-X integration within the collagenous network. *FEBS Lett.* **580**, 6281–6285.
19. Elefteriou, F., Exposito, J. Y., Garrone, R. & Lethias, C. (2001). Binding of tenascin-X to decorin. *FEBS Lett.* **495**, 44–47.
20. Zweers, M. C., van Vlijmen-Willems, I. M., van Kuppevelt, T. H., Mecham, R. P., Steijlen, P. M., Bristow, J. & Schalkwijk, J. (2004). Deficiency of tenascin-X causes abnormalities in dermal elastic fiber morphology. *J. Invest. Dermatol.* **122**, 885–891.
21. Burch, G. H., Gong, Y., Liu, W., Dettman, R. W., Curry,

C. J., Smith, L. *et al.* (1997). Tenascin-X deficiency is associated with Ehlers–Danlos syndrome. *Nat. Genet.* **17**, 104–108.
22. Elefteriou, F., Exposito, J. Y., Garrone, R. & Lethias, C. (1997). Characterization of the bovine tenascin-X. *J. Biol. Chem.* **272**, 22866–22874.
23. Rief, M., Gautel, M., Oesterhelt, F., Fernandez, J. M. & Gaub, H. E. (1997). Reversible unfolding of individual titin immunoglobulin domains by AFM. *Science*, **276**, 1109–1112.
24. Marko, J. F. & Siggia, E. D. (1995). *Macromolecules*, **28**, 8759–8770.
25. Oberhauser, A. F., Badilla-Fernandez, C., Carrion-Vazquez, M. & Fernandez, J. M. (2002). The mechanical hierarchies of fibronectin observed with single-molecule AFM. *J. Mol. Biol.* **319**, 433–447.
26. Carrion-Vazquez, M., Oberhauser, A. F., Fowler, S. B., Marszalek, P. E., Broedel, S. E., Clarke, J. & Fernandez, J. M. (1999). Mechanical and chemical unfolding of a single protein: a comparison. *Proc. Natl Acad. Sci. USA*, **96**, 3694–3699.
27. Cao, Y. & Li, H. (2007). Polyprotein of GB1 is an ideal artificial elastomeric protein. *Nat. Mater.* **6**, 109–114.
28. Peng, Q. & Li, H. (2008). Atomic force microscopy reveals parallel mechanical unfolding pathways of T4 lysozyme: evidence for a kinetic partitioning mechanism. *Proc. Natl Acad. Sci. USA*, **105**, 1885–1890.
29. Lethias, C., Elefteriou, F., Parsiegla, G., Exposito, J. Y. & Garrone, R. (2001). Identification and characterization of a conformational heparin-binding site involving two fibronectin type III modules of bovine tenascin-X. *J. Biol. Chem.* **276**, 16432–16438.
30. Lethias, C., Descollonges, Y., Boutillon, M. M. & Garrone, R. (1996). Flexilin: a new extracellular matrix glycoprotein localized on collagen fibrils. *Matrix Biol.* **15**, 11–19.
31. Krammer, A., Lu, H., Isralewitz, B., Schulten, K. & Vogel, V. (1999). Forced unfolding of the fibronectin type III module reveals a tensile molecular recognition switch. *Proc. Natl Acad. Sci. USA*, **96**, 1351–1356.
32. Craig, D., Gao, M., Schulten, K. & Vogel, V. (2004). Tuning the mechanical stability of fibronectin type III modules through sequence variations. *Structure*, **12**, 21–30.
33. Gao, M., Craig, D., Lequin, O., Campbell, I. D., Vogel, V. & Schulten, K. (2003). Structure and functional significance of mechanically unfolded fibronectin type III1 intermediates. *Proc. Natl Acad. Sci. USA*, **100**, 14784–14789.
34. Wright, C. F., Teichmann, S. A., Clarke, J. & Dobson, C. M. (2005). The importance of sequence diversity in the aggregation and evolution of proteins. *Nature*, **438**, 878–881.
35. Oberhauser, A. F., Marszalek, P. E., Carrion-Vazquez, M. & Fernandez, J. M. (1999). Single protein misfolding events captured by atomic force microscopy. *Nat. Struct. Biol.* **6**, 1025–1028.